Parasitology International 65 (2016) 539–544

Contents lists available at ScienceDirect

Parasitology International

journal homepage: www.elsevier.com/locate/parint

# Detailed methodology for high resolution scanning electron microscopy (SEM) of murine malaria parasitized-erythrocytes

Eri H. Hayakawa *, Hiroyuki Matsuoka

*Division of Medical Zoology, Department of Infection and Immunity, Jichi Medical University, Yakushiji 3311-1, Shimotsuke, Tochigi 329-0498, Japan*

ARTICLE INFO

*Article history:*
Received 6 November 2015
Received in revised form 1 March 2016
Accepted 13 March 2016
Available online 15 March 2016

*Keywords:*
Scanning electron microscopy (SEM)
Mouse erythrocyte
*Plasmodium berghei*
*Plasmodium yoelii*
*Plasmodium chabaudi*
*Plasmodium falciparum*

ABSTRACT

Scanning electron microscopy (SEM) is a powerful tool used to investigate object surfaces and has been widely applied in both material science and biology. With respect to the study of malaria, SEM revealed that erythrocytes infected with *Plasmodium falciparum*, a human parasite, display 'knob-like' structures on their surface comprising parasitized proteins. However, detailed methodology for SEM studies of malaria parasites is lacking in the literature making such studies challenging. Here, we provide a step-by-step guide to preparing *Plasmodium*-infected erythrocytes from two mouse strains for SEM analysis with minimal structural deterioration. We tested three species of murine malaria parasites, *P. berghei*, *P. yoelii*, and *P. chabaudi*, as well as non-parasitized human erythrocytes and *P. falciparum*-infected erythrocytes for comparisons. Our data demonstrated that the surface structures of parasitized erythrocytes between the three species of murine parasites in the two different strains of mice were indistinguishable and no surface alterations were observed in *P. falciparum*-erythrocytes. Our SEM observations contribute towards an understanding of the molecular mechanisms of parasite maturation in the erythrocyte cytoplasm and, along with future studies using our detailed methodology, may help to gain insight into the clinical phenomena of human malaria.


## 1. Background

Malaria is an infectious disease caused by parasitic protozoan of the genus *Plasmodium*, which invade erythrocytes. Infected erythrocytes undergo a variety of cellular alterations. For example, *Plasmodium falciparum*-infected erythrocytes display anemia [1], and changes in the erythrocyte membrane that affect cell adhesion properties [2–4], the cytoskeletal structure [5], lipid-protein interactions [6], and hemichrome attachment [7], along with accelerated band 3 clustering [7] and hemozoin formation [8,9]. These changes are mainly caused by the expression of parasitized proteins intracellularly in erythrocytes, and alterations on the erythrocyte surface can lead to evasion of parasites from anti-oxidation by heme after hemoglobin is digested by the parasites. Parasitized proteins of *P. falciparum* affect not only intracellular erythrocyte structures but also surface structures on erythrocytes, known as Knob proteins. Knob is an interconnected protein complex predominantly comprising PfEMP-1, KAHRP, and PfEMP-3. This interaction with the knob protein complex leads to adhesion of infected erythrocytes to capillary blood vessels of the brain and the induction of cerebral malaria.

Malaria has been reported not only in humans but also in primates [10,11], rodents [12–14], avian species [15,16], and reptiles [17–19]. "Knob-like" structures have been observed on the surfaces of *Plasmodium fragile* and *Plasmodium coatneyi*-infected erythrocytes, species of *Plasmodium* responsible for malaria in monkeys [20–22]. However, there is little information regarding the relationship between altered surface structures on parasitized-erythrocytes and (clinical) symptoms in different host animals.

Rodent malaria protozoa, *Plasmodium berghei*, *Plasmodium yoelii*, and *Plasmodium chabaudi*, have been studied as human malaria models. However, the genes encoding PfEMP-1 and KAHRP are not present in these three species of parasites, with the closest homolog being PfEMP-3 (PlasmoDB) in *P. yoelii*, which may encode a partial or full-length protein. Balb/cCrS1c (BALB/c) and C57 BL/6NCrS1c (C57BL/6) mice are well established models for malaria parasite infection. However, these mouse species have distinct immune systems and may therefore respond differently to malarial parasites. Thus, it is important to investigate the properties of parasitized erythrocytes in different combinations of parasite and host animal as comparative studies.

Scanning electron microscope (SEM) is a powerful tool for the observation of surface structures with high spatial resolution. This technique enabled the discovery that *P. falciparum*-infected erythrocytes display altered surface structures [23,24], which was found to be due to

* Corresponding author.
*E-mail address:* erihayakawa@jichi.ac.jp (E.H. Hayakawa).

http://dx.doi.org/10.1016/j.parint.2016.03.006

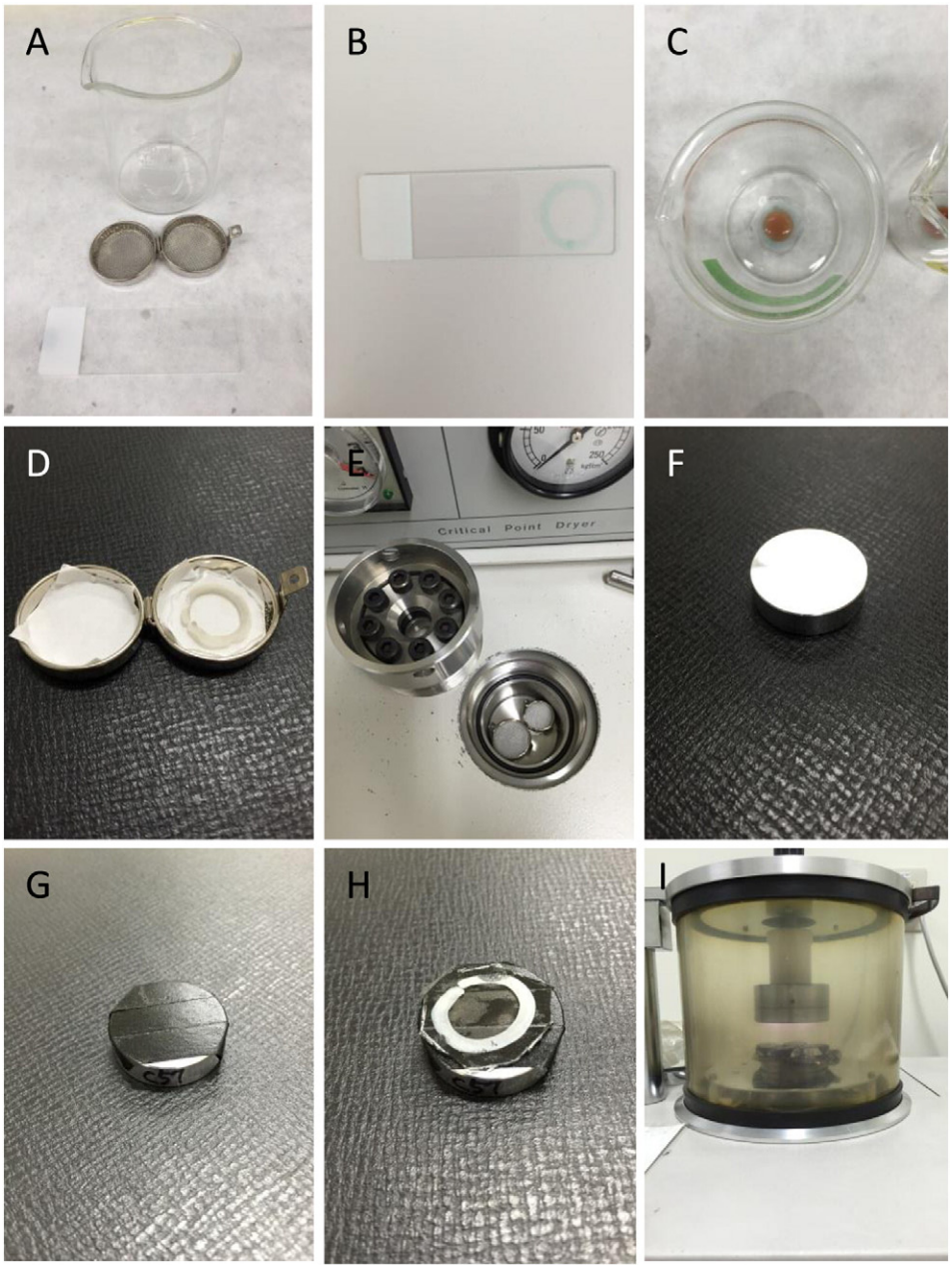


**Fig. 1.** Apparatus required for sample preparation for SEM observation. The size of the slide was adjusted to fit the basket and beaker (A). The sample area was marked with pen on a glass microslide (B). Erythrocytes in buffer were spread onto the slide. A higher concentration of erythrocytes was preferable, as shown, rather than using erythrocytes fixed in 2% GA (C). A size-adjusted paper filter was placed in the basket (D), then the dehydrated sample was placed on top. The closed basket was immediately placed into ethanol/isoamyl acetate. The temperature of the equipment was set 10 °C below room temperature, and the basket was placed into the chamber (E). A sample holder for the glass sample is shown (F). Carbon tape was required to fix the sample holder and the glass sample in place (G, H). The sample was sputtered using Pt-Pd; 15 mV for 60 s was sufficient for our sample (I).

parasitized proteins altering the erythrocyte cytoskeleton and lipid-protein interactions at the erythrocyte membrane. Electron microscopy imaging has long been used in various scientific fields and more recent studies therefore only describe simplified material preparation methods. The intricacies of sample preparation procedures required to replicate experiments are often overlooked.

## 2. Objectives

To provide a comprehensive step-by-step description of the sample preparation procedure for SEM imaging to clearly visualize the morphology of suspended cells of non-parasitized and parasitized erythrocytes. In addition, to compare the erythrocyte surface topography in two different host mouse models (C57BL/6 and BALB/c) infected with three different species of malaria parasites (*P. yoelii*, *P. berghei*, and *P. chabaudi*).

## 3. Methods

### *3.1. Sample preparation for SEM*

(1) Non-parasitized or parasitized erythrocytes (6–12 μL) were fixed with 1–4% paraformaldehyde (PFA) in 0.1 mol/L HEPES buffer (pH 7.4) (1 mL), which had been filtered through a 0.22 μm-bottle top filter (Corning, NY, USA), and were immediately mixed by vortexing for 5 min. In our experience, loss of structural integrity is often observed when PFA is used alone at a concentration of 4%. Fixation with 2% PFA and/or 1–2% glutaraldehyde (GA)

is preferable for maintaining structural integrity in electron microscopy sample preparations; we therefore employed 2% PFA in this study and did not observe morphological evidence of structural damage. The concentration of PFA should be optimized for different materials and experimental conditions.

(2) Samples were immediately placed on ice for 5 min, then vortexed for 5 min. This step was repeated for at least 1 h, with optimal fixation occurring after 2 h. The cooling and vortexing steps can be extended to 10–15 min.

(3) Samples were washed with 0.1 mol/L HEPES buffer (pH 7.4) at least three times after fixation.

(4) At this stage, samples could be stored for up to 1 month at 4 °C.

(5) An MAS-coated glass microslide (S9441; Matsunami Glass Ind., Ltd., Kishiwada, Osaka, Japan) was cut to size using a diamond cutter (Fig. 1A). The sample area was marked with Liquid Blocker (Daido Sangyo Co., Ltd., Tokyo, Japan) (Fig. 1B), and the size of the glass was adjusted to fit the basket.

(6) After cutting, the glass was placed into a 100 mL beaker and the erythrocyte solution was spread onto the marked area on the glass (Fig. 1C).

(7) The glass was incubated for 10 min at room temperature for immobilization of the cells.

(8) The glass was then washed with phosphate buffer (pH 7.4, 0.1 mol/L) three times.

(9) The samples were further fixed with 2% osmium tetroxide (Nisshin EM Co., Tokyo, Japan) in phosphate-buffered saline (pH 7.4, 0.2 mol/L) (1:1 vol/vol) for 30–60 min at room temperature (final osmium concentration: 1%), then dehydrated with 70% ethanol.

(10) After aspirating the 70% ethanol, 80% ethanol was added to the samples for 10–20 min, followed by repeated dehydration steps with increasing concentrations of ethanol (90%, 95%, and finally 100% twice).

(11) The samples were then soaked in 100% ethanol and isoamyl acetate mixture (1:1 vol/vol) (Wako, Osaka, Japan).

(12) A size-adjusted paper filter was placed in the basket and the glass sample was placed on the paper (Fig. 1D). The basket was closed and placed in ethanol/isoamyl acetate to avoid drying of the sample surface.

(13) The sample basket was placed into the chamber of a critical point dryer HCP-2 (Dryer HCP-2, Hitachi Koki Co., Ltd., Tokyo, Japan). Excess isoamyl acetate was then washed out with liquid $CO_2$ three times. Then, liquid $CO_2$ (60–80%) was infused into the chamber and samples were incubated for 20 min at 20 °C to allow the isoamyl acetate to diffuse (Fig. 1E).

(14) The temperature was raised to 40 °C for 5 min, then the liquid $CO_2$ was leaked and the sample was dried at the critical point temperature for ~20 min.

(15) The basket/sample was mounted on a sample holder, which was then covered with carbon tape (Fig. 1F, G).

(16) The sample was sputtered using an Ion Sputter (E-1030, Hitachi, Ltd., Tokyo, Japan) with the Pt-Pd at 15 mV for 60 s (Fig. 1H, I).

(17) Sample observations were performed using an S-4300 scanning electron microscope (Hitachi High-Technologies Corporation, Tokyo, Japan).

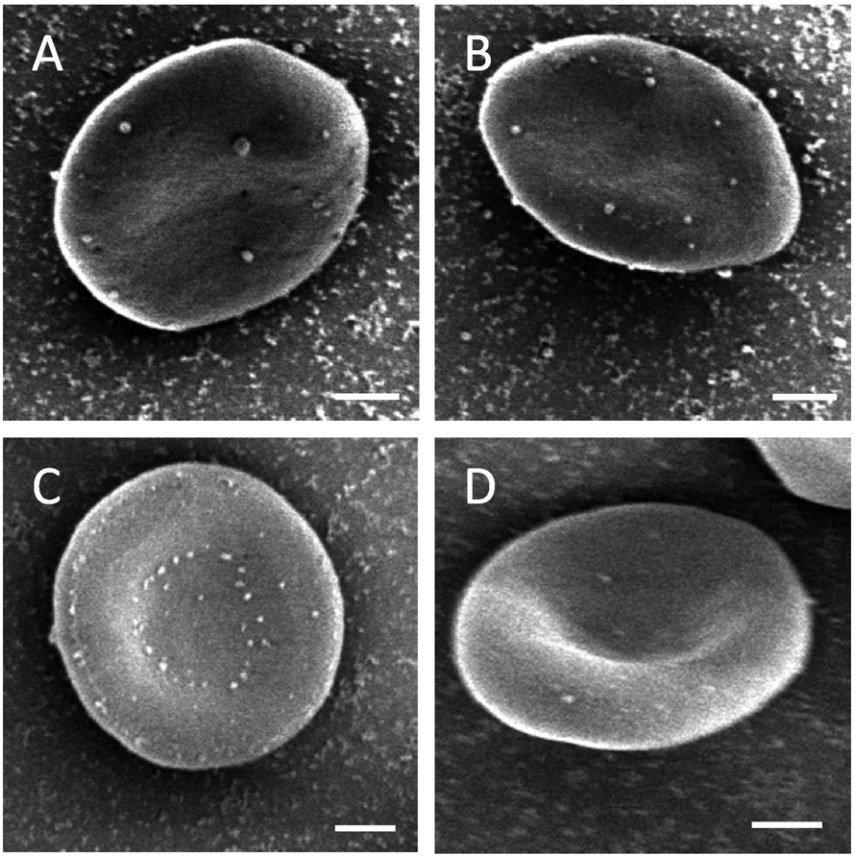


**Fig. 2.** SEM imaging data of non-parasitized erythrocytes of C57BL/6 (A, B) and BALB/c (C, D) mice. Bar = 1.0 μm.

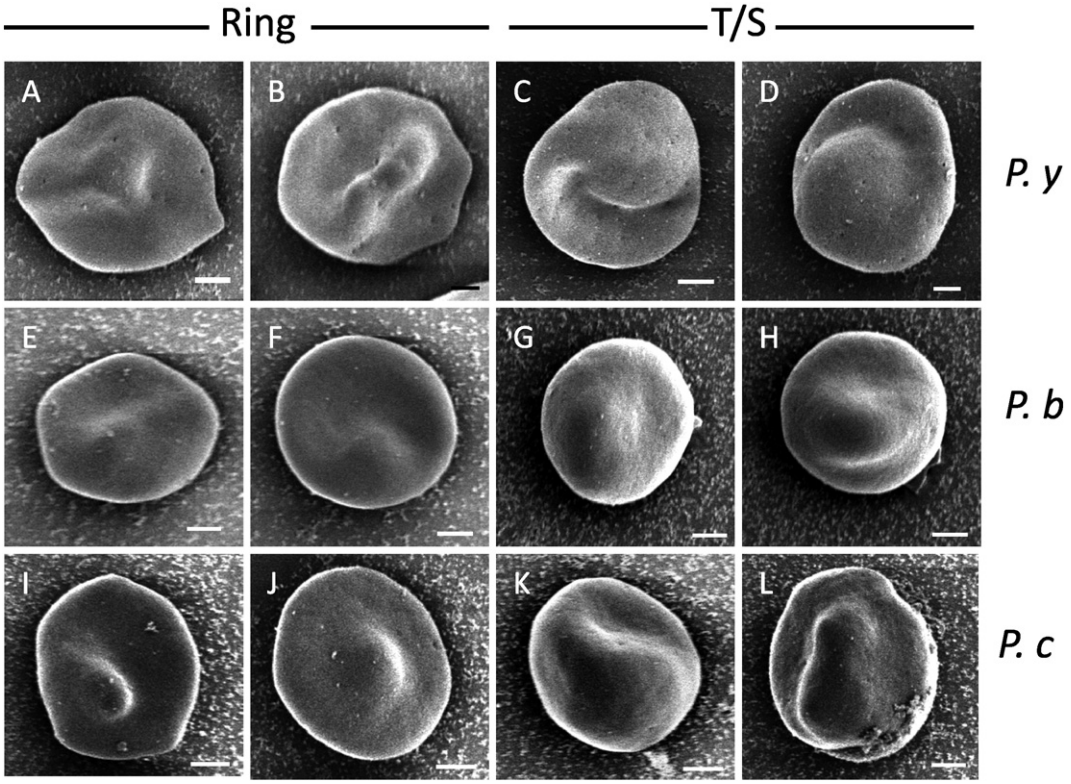


**Fig. 3.** SEM imaging of *P. yoelii*-, *P. berghei*-, and *P. chabaudi*-infected erythrocytes in C57BL/6 mice. Bar = 1.0 μm.

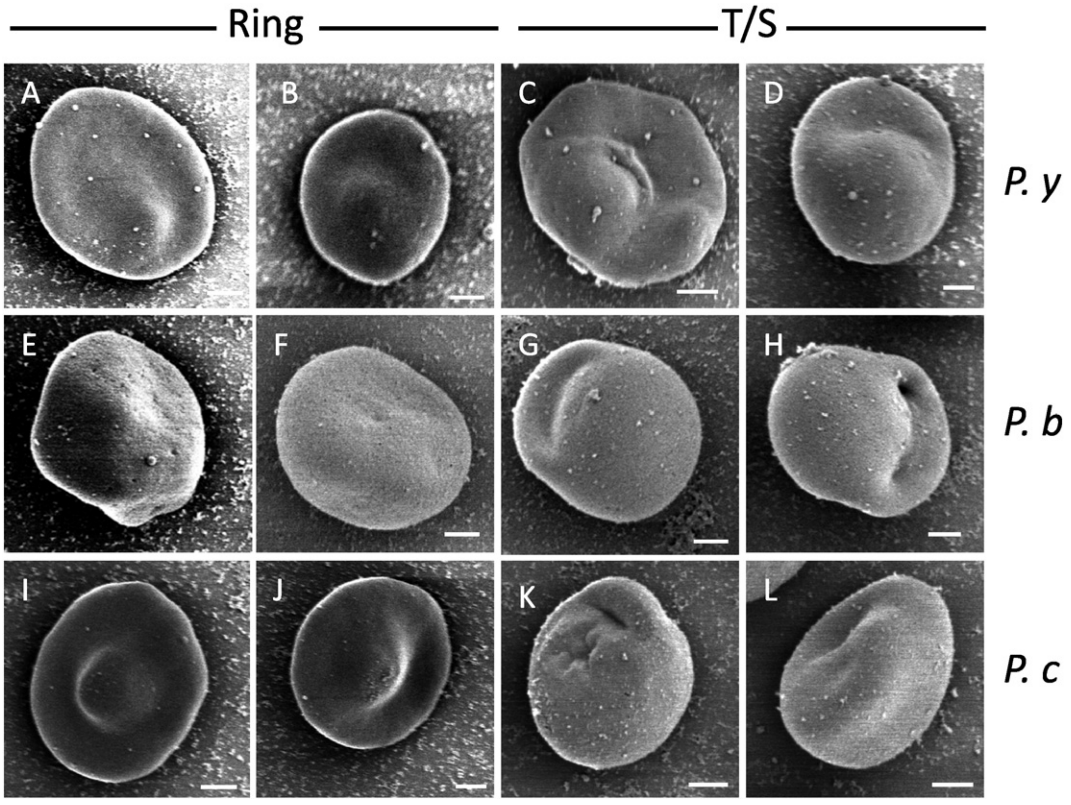


**Fig. 4.** SEM imaging of *P. yoelii*, *P. berghei*, and *P. chabaudi*-infected erythrocytes in BALB/c mice. The existence and localization of parasites is clearly shown in the ring and trophozoite/schizont stage. Bar = 1.0 μm.

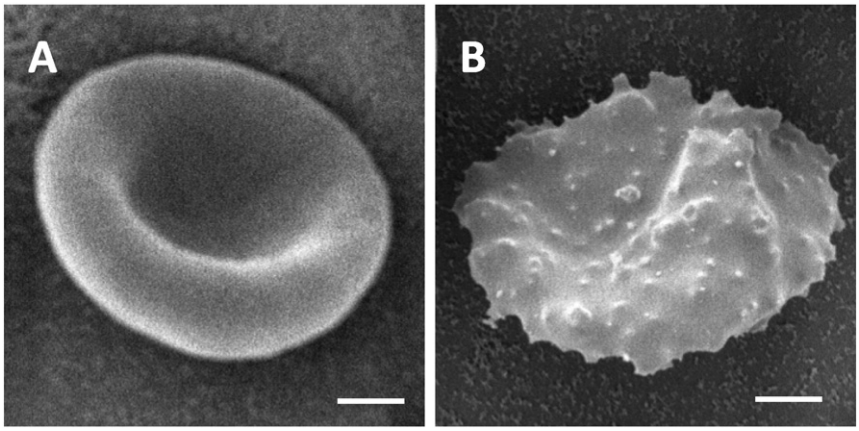


**Fig. 5.** Non-parasitized and *P. falciparum*-infected human erythrocytes. A smooth surface topography was observed with the non-parasitized erythrocytes (A), compared with a raised 'knob-like' structure on the *P. falciparum*-infected human erythrocyte membrane (B). Bar = 1.0 μm.

## 4. Special remarks/comments

### *4.1. Comparison of three species of murine parasitized erythrocytes in two different strains of mice and P. falciparum infected-erythrocytes by SEM*

SEM imaging successfully demonstrated the characteristic topography of the murine parasitized-erythrocyte surface with high resolution. SEM images of non-parasitized erythrocytes from C57BL/6 (A, B) and BALB/c (C, D) mice are shown in Fig. 2. A smooth surface membrane was observed with no significant differences between erythrocytes from the two mouse strains.

Fig. 3 shows C57BL/6 erythrocytes. Images A–D show *P. yoelii*-infected erythrocytes, images E–H show *P. berghei*-infected erythrocytes, and images I–L show *P. chabaudi*-infected erythrocytes. There were no knob or 'knob-like' structures observed on the surface of the erythrocytes in the ring-trophozoite-schizont stages in the three different parasites. Different sizes of internal parasites were observed according to the growth of the parasites. Fig. 4 shows BALB/c mouse erythrocytes. The ring stage of the parasitized erythrocytes is shown in images A, B, E, F, I, and J. The trophozoite/schizont stages of parasitized erythrocytes are shown in images C, D, G, H, K, and L. In the case of BALB/c mice, we did not observe any raised structures, such as those resembling knob or 'knob-like' structures, on the erythrocyte membranes. We observed increases in parasite size in host erythrocytes infected with *P. yoelii*, *P. berghei*, and *P. yoelii*, as seen in C57BL/6 mice. These SEM imaging results clearly differed from those obtained with *P. falciparum*-infected erythrocytes (Fig. 5B), which displayed a knob structure.

In *P. yoelii*, PfEMP-3 (PlasmoDB) encodes a partial or full-length protein, which distinguishes it from *P. berghei* and *P. chabaudi*. However, none of these three species displayed a Knob structure on infected erythrocytes (Figs. 3 and 4), consistent with the fact that all three species lack PfEMP-1, a member of the *var.* multiple family. When comparing C57BL/6 with BALB/c mouse erythrocytes infected with the same parasites (Figs. 3 and 4), no significant differences were observed on the erythrocyte surfaces. Differences identified between the immune systems of these mice do not therefore appear to directly affect parasitized protein expression and localization.

Mouse malaria has been widely studied as a model of human malarial infection. However, the mouse malaria-infected erythrocytes used in this study did not display knob structures known to mediate adhesion to endothelial cells. This raises the question of how mouse malaria-parasitized erythrocytes may be applicable for a human malaria model, especially for *P. falciparum* infection. Hecht et al. reported, in C57BL/6 mice, age-dependent collateral vasculature and cerebrovascular remodeling resulting in stroke [25]. These age-dependent effects may also play a part in the mouse malaria model since a greater inflammatory reaction was observed after invasion of erythrocytes in older mice than in younger mice. This inflammatory reaction induced a cytokine storm reducing parasitemia in mice and the surviving parasitized-erythrocytes sequestered in the lung and liver evading the bloodstream. Similar findings were reported by Waisberg et al. [26] and are probably applicable to not only C57BL/6 mice but also BALB/c mice and other strains. In summary, we report that knobless *P. berghei*, *P. yoelii*, and *P. chabaudi*-infected erythrocytes do not mediate infraction in (capillary) blood vessels, and may not cause brain infarction. However, we believe that the mouse model of malaria can provide important insight into mechanisms to evade cerebral malaria that could be potentially adapted for human therapeutic benefit.

### *4.2. Sample correction and isolation of parasitized erythrocytes*

The host animals used in this study were 6–8-week-old female Balb/cCrS1c (BALB/c) and C57 BL/6NCrS1c (C57BL/6) mice (Japan SLC, Hamamatsu, Shizuoka, Japan). All animal procedures were approved by the Animal Ethics Committee of Jichi Medical University, Japan. Both strains of mice were infected with *P. berghei*, *P. yoelii*, and *P. chabaudi*. After mice had been bitten by a malaria-infected mosquito (*Anopheles stephensi*), blood that included nonparasitized- and parasitized-erythrocytes (=phase zero) were collected from the mice.

Human erythrocytes ($O^+$ blood type) for *P. falciparum* culture (3D7) were obtained from the Japanese Red Cross Society (authorization number: 25J-0045). *P. falciparum* culture was performed as described in our previous study [27]. Briefly, non-parasitized erythrocytes were washed three times with incomplete RPMI medium [RPMI 1640 (Invitrogen Life Technologies, Grand Island, NY, USA) medium containing 0.367 μmol/L hypoxanthine (Sigma, St. Louis, MO, USA), 25 μmol/L sodium bicarbonate (Invitrogen), 25 μmol/L HEPES (Sigma), and 10 μg/mL gentamicin (Invitrogen)]. At this stage, non-parasitized erythrocytes could be stored at 50% hematocrit (Ht) in incomplete RPMI 1640 for 1–2 weeks at 4 °C until use. For *P. falciparum* parasite culture, the erythrocyte suspension was adjusted to 3% hematocrit (Ht) in complete RPMI [incomplete RPMI 1640 plus 10 mg/mL AlbuMAX® II Lipid-Rich BSA (Invitrogen Life Technologies)] and incubated in an atmosphere of 90% $N_2$/5% $CO_2$/5% $O_2$ at 37 °C.

The non-parasitized erythrocytes/ring stage and the trophozoite/schizont stage of human/mouse erythrocytes were separated using MACS Separators LS columns (Miltenyi Biotec K.K., Bergisch Gladbach, Germany) [27]. Then, all erythrocytes were subjected to sample preparation for SEM.

## Acknowledgements

E.H.H. was partially supported by JSPS KAKENHI (Grant-in-Aid for Scientific Research (C), grant number 24500992).

## References

[1] L.H. Miller, H.C. Ackerman, X.Z. Su, T.E. Wellems, Malaria biology and disease pathogenesis: insights for new treatments, Nat. Med. 19 (2013) 156–167.
[2] M. Avril, Inhibition of infected red blood cell binding to the vascular endothelium, Methods Mol. Biol. 1325 (2015) 215–229.
[3] P.A. Carvalho, M. Diez-Silva, H. Chen, M. Dao, S. Suresh, Cytoadherence of erythrocytes invaded by *Plasmodium falciparum*: quantitative contact-probing of a human malaria receptor, Acta Biomater. 9 (2013) 6349–6359.
[4] B.S. Crabb, B.M. Cooke, J.C. Reeder, R.F. Waller, S.R. Caruana, K.M. Davern, et al., Targeted gene disruption shows that knobs enable malaria-infected red cells to cytoadhere under physiological shear stress, Cell 89 (1997) 287–296.
[5] S. Das, N. Hertrich, A.J. Perrin, C. Withers-Martinez, C.R. Collins, M.L. Jones, et al., Processing of *Plasmodium falciparum* merozoite surface protein MSP1 activates a spectrin-binding function enabling parasite egress from RBCs, Cell Host Microbe 18 (2015) 433–444.
[6] J. Garcia, H. Curtidor, C.G. Pinzon, M. Vanegas, A. Moreno, M.E. Patarroyo, Identification of conserved erythrocyte binding regions in members of the *Plasmodium falciparum* Cys6 lipid raft-associated protein family, Vaccine 27 (2009) 3953–3962.
[7] G. Giribaldi, D. Ulliers, F. Mannu, P. Arese, F. Turrini, Growth of *Plasmodium falciparum* induces stage-dependent haemichrome formation, oxidative aggregation of band 3, membrane deposition of complement and antibodies, and phagocytosis of parasitized erythrocytes, Br. J. Haematol. 113 (2001) 492–499.
[8] K. Kim, H. Yoon, M. Diez-Silva, M. Dao, R.R. Dasari, Y. Park, High-resolution three-dimensional imaging of red blood cells parasitized by *Plasmodium falciparum* and in situ hemozoin crystals using optical diffraction tomography, J. Biomed. Opt. 19 (2014) 011005.
[9] K. Bendrat, B.J. Berger, A. Cerami, Haem polymerization in malaria, Nature 378 (1995) 138–139.
[10] R. Mason Dentinger, Patterns of infection and patterns of evolution: how a malaria parasite brought "monkeys and man" closer together in the 1960s, J. Hist. Biol. (2015), http://dx.doi.org/10.1007/s10739-015-9421-8 (Epub ahead of print).
[11] K. Tyagi, D. Gupta, E. Saini, S. Choudhary, A. Jamwal, M.S. Alam, et al., Recognition of human erythrocyte receptors by the tryptophan-rich Antigens of monkey malaria parasite *Plasmodium knowlesi*, PLoS One 10 (2015), e0138691.
[12] M.A. Dkhil, S. Al-Quraishy, A. Al-Shamrany, A.S. Alazzouni, M.Y. Lubbad, E.M. Al-Shaebi, et al., Protective effect of berberine chloride on *Plasmodium chabaudi*-induced hepatic tissue injury in mice, Saudi J. Biol. Sci. 22 (2015) 551–555.
[13] M. Canavese, T. Dottorini, A. Crisanti, VEGF and LPS synergistically silence inflammatory response to *Plasmodium berghei* infection and protect against cerebral malaria, Pathog. Glob. Health 109 (2015) 255–265.
[14] J.L. Grun, W.P. Weidanz, Immunity to *Plasmodium chabaudi* adami in the B-cell-deficient mouse, Nature 290 (1981) 143–145.
[15] R. Pigeault, J. Vezilier, S. Cornet, F. Zele, A. Nicot, P. Perret, et al., Avian malaria: a new lease of life for an old experimental model to study the evolutionary ecology of Plasmodium, Philos. Trans. R Soc. Lond. B Biol. Sci. 370 (2015).
[16] S. Pattaradilokrat, W. Tiyamanee, P. Simpalipan, M. Kaewthamasorn, T. Saiwichai, J. Li, et al., Molecular detection of the avian malaria parasite *Plasmodium gallinaceum* in Thailand, Vet. Parasitol. 210 (2015) 1–9.
[17] A.T. Neal, Male gametocyte fecundity and sex ratio of a malaria parasite, *Plasmodium mexicanum*, Parasitology 138 (2011) 1203–1210.
[18] S.C. Ayala, Lizard malaria in California; description of a strain of *Plasmodium mexicanum*, and biogeography of lizard malaria in western North America, J. Parasitol. 56 (1970) 417–425.
[19] S.C. Ayala, D. Lee, Saurian malaria: development of sporozoites in two species of phlebotomine sandflies, Science 167 (1970) 891–892.
[20] C.D. Smith, A.E. Brown, S. Nakazawa, H. Fujioka, M. Aikawa, Multi-organ erythrocyte sequestration and ligand expression in rhesus monkeys infected with *Plasmodium coatneyi* malaria, Am.J.Trop. Med. Hyg. 55 (1996) 379–383.
[21] R. Udomsangpetch, A.E. Brown, C.D. Smith, H.K. Webster, Rosette formation by *Plasmodium coatneyi*-infected red blood cells, Am.J.Trop. Med. Hyg. 44 (1991) 399–401.
[22] H. Fujioka, P. Millet, Y. Maeno, S. Nakazawa, Y. Ito, R.J. Howard, et al., A nonhuman primate model for human cerebral malaria: rhesus monkeys experimentally infected with *Plasmodium fragile*, Exp. Parasitol. 78 (1994) 371–376.
[23] M. Aikawa, Human cerebral malaria, Am.J.Trop. Med. Hyg. 39 (1988) 3–10.
[24] E.H. Hayakawa, S. Kobayashi, H. Matsuoka, Physicochemical aspects of the *Plasmodium chabaudi*-infected erythrocyte, Biomed Res Int. 2015 (2015), 642729.
[25] N. Hecht, J. He, I. Kremenetskaia, M. Nieminen, P. Vajkoczy, J. Woitzik, Cerebral hemodynamic reserve and vascular remodeling in C57/BL6 mice are influenced by age, Stroke 43 (2012) 3052–3062.
[26] M. Waisberg, T. Tarasenko, B.K. Vickers, B.L. Scott, L.C. Willcocks, A. Molina-Cruz, et al., Genetic susceptibility to systemic lupus erythematosus protects against cerebral malaria in mice, Proc. Natl. Acad. Sci. U. S. A. 108 (2011) 1122–1127.
[27] E.H. Hayakawa, F. Tokumasu, J. Usukura, H. Matsuoka, T. Tsuboi, T.E. Wellems, Imaging of the subsurface structures of "unroofed" *Plasmodium falciparum*-infected erythrocytes, Exp. Parasitol. 153 (2015) 174–179.